

High-Pressure Raman Study of Anthracene

Liang Zhao, Bruce J. Baer, and Eric L. Chronister*

Department of Chemistry, University of California at Riverside, Riverside, California 92521

Received: August 10, 1998; In Final Form: December 18, 1998

Pressure-induced Raman shifts and line broadening in crystalline anthracene have been studied up to 3.1 GPa at ambient temperature. The use of nitrogen as a hydrostatic pressure medium eliminated pressure-induced defect fluorescence that had previously restricted high-pressure Raman studies of anthracene. Mode Grüneisen parameters have been determined for six phonons and nine vibrons, and some evidence for a previously suggested phase transition at 2.4 ± 0.2 GPa is observed in the line width data. The calibrated pressure-induced spectral shifts and line width changes also can be utilized as a gauge of the pressure and temperature profile of a laser-induced shock front (Hambir, S. A.; Franken, J.; Hare, D. E.; Chronister, E. L.; Baer, B. J.; Dlott, D. D. *J. Appl. Phys.* **1997**, *81*, 2157).

1. Introduction

High-pressure vibrational spectroscopy is a useful tool for examining intermolecular interactions and dynamics in molecular solids.^{1,2,3} Changes in the vibrational spectrum can be used to probe chemical and physical changes associated with static high pressure¹ as well as detonation reactions and shock chemistry in molecular solids.⁴ The time-resolved pressure and temperature changes associated with a shock wave not only lead to complicated spectral changes, but also shock wave energy can be coupled into intramolecular vibrations of crystallites doped into a polymer host.⁵ When the Hugoniot is known the density can be converted to shock pressure.⁶ Although density and temperature effects can in principle be calculated from a detailed knowledge of the anharmonic intermolecular potential^{7,8} static high-pressure Raman studies of molecular crystals can be used to empirically calibrate pressure-induced spectral changes for analysis of shock-induced spectral changes.⁹ For example, time-resolved shifts in the 1403 cm^{-1} Raman transition of anthracene (ambient pressure) has proven useful for probing the temperature and pressure profile of laser-induced shock waves in organic polymer materials.⁹ The present study examines pressure-induced frequency shifts and line broadening for 15 Raman modes of crystalline anthracene. Some of the lower-frequency Raman modes have pressure-induced Raman shifts five times that of the 1403 cm^{-1} band previously used as a shock wave pressure gauge.⁹

Anthracene is a model molecular crystal system¹⁰ for which the isothermal compressibility,¹¹ the Hugoniot,¹² and a variety of other physical properties¹⁰ and spectroscopic data are available in the literature. In addition, the totally symmetric vibrations of crystalline anthracene have large Raman cross-sections and narrow intrinsic line widths,¹³ which facilitates the measurement of frequency shifts and line broadening effects.¹⁴

There have been few investigations of the vibrational spectra of the internal modes of polyacenes at high pressure^{8,15,16} since earlier Raman studies of anthracene and naphthalene at high pressure reported a large fluorescence background attributed to excimer-like emission from crystalline defects.¹⁵ For anthracene crystals it was reported that pressure-induced excimer defect

emission dominated the Raman spectrum at pressures greater than 1.7 GPa.¹⁵ There have also been previous Raman studies of the phonon modes of anthracene at pressures below 1 GPa.^{8,17} Although infrared studies of anthracene have been made at high pressure,¹⁶ the IR active modes and the Raman active modes are mutually exclusive due to the inversion symmetry of the crystal.

The crystal structure of anthracene is monoclinic (Space group $P2_1/a$), which is typical of polyacenes. There are two equivalent molecules per unit cell with site symmetry C_i . The site group C_i is a subgroup of both the molecular point group (D_{2h}) and the crystal factor group (C_{2h}) and provides a correlation between these groups.^{18,19} Thus, in the anthracene crystal all vibronic modes are either Raman active or IR active.

An IR study has yielded some evidence for a second-order or weakly first-order phase transition at 2.4 ± 0.2 GPa.¹⁶ In that study, discontinuities in the pressure shift and changes in the rate of shift versus pressure were reported at the transition pressure. It was suggested that the higher pressure phase had crystal symmetry $P1$ and that the two molecules per unit cell were each independent centers of symmetry. The samples in that study used Nujol as the pressure medium. Despite the crystallization of Nujol at 1.3 GPa, the pressures were believed to be hydrostatic.¹⁶

In the present study, the use of fluid nitrogen as a hydrostatic pressure medium has alleviated defect fluorescence enabling us to obtain fluorescence-free Raman spectra at high pressure. In this study we have catalogued the effect of pressure on the frequency and line width of six phonons and nine vibrons of crystalline anthracene, and determined mode Grüneisen data for all of these vibrational modes. These results can increase the precision with which anthracene microcrystals can be used as a pressure and temperature gauge in time-resolved spectroscopic studies of shock fronts.⁹ The results of this study are also used to evaluate the proposed second-order anthracene phase transition at 2.4 GPa.¹⁶

2. Experimental Section

Zone-refined anthracene with a purity of 99+% (Aldrich product number 33,148-1) was used for this study. Large crystals were shattered into microcrystals ($\sim 20\text{ }\mu\text{m}$ diameter) and

* Author to whom correspondence should be addressed.

typically dozens of these microcrystals were loaded into the high-pressure cell. A diamond anvil cell of the Merrill–Bassett design,²⁰ with a diamond culet size of 1 mm, was used for generating pressures to approximately 3 GPa. The gaskets were made from 0.25 mm thick Inconel 750 and had an aperture of 0.5 mm. The sample volume was half-filled with anthracene microcrystals along with a few ruby chips, and the remaining volume was filled with liquid nitrogen by the immersion technique.²¹ Although nitrogen freezes at 2.4 GPa, it is a plastic crystal at ambient temperature and provides an excellent hydrostatic medium at all pressures in this study.

Excitation with the 514.5 nm Ar⁺ laser line was used to obtain Raman spectra as well as ruby luminescence^{22,23} pressure measurements. All spectra were obtained at ambient temperature 24 ± 2 °C. Over the range of this study, the R₁ line of the ruby shifts at a near constant 7.56 cm⁻¹ per GPa,^{22,23} resulting in sample pressures determined to a precision of ±0.03 GPa. The Raman shifts were reproducible within the precision of the pressure measurement. The high-pressure Raman spectra were obtained by varying the pressure nonmonotonically. In addition, the high-pressure Raman data was obtained for several different samples loaded into the same cell. The random order of the pressure changes did not result in hysteresis in either the observed frequencies or line widths. Raman spectra were collected in a near 180° backscattering geometry over a frequency range from 50 to 1800 cm⁻¹. We did not resolve narrow lines for the C–H stretches. A scanning double monochromator with 2400 groove/mm gratings was employed with a spectral resolution of 1 cm⁻¹. Data acquisition was automated using a modified version of a program provided by D. Schiferl (CST-6 Los Alamos National Laboratory).²⁴ Ruby peak positions were obtained from a fit of two Lorentzian peaks. The Raman peaks corresponding to intramolecular vibrations were best fit by Gaussian line shapes, while the phonon modes were best fit by Lorentzian line shapes. The signal-to-noise did not warrant fitting the data to Voigt line shapes. A χ² analysis was used to determine the best fit of the line shape to the data, and nonlinear least-squares fitting was used to determine the statistical error for the resulting frequency and line width parameters.²⁵

3. Vibrational Frequency Shifts upon Compression

The pressure-induced compression of anthracene has been fit using the Murnaghan equation:¹¹

$$P = \left(\frac{B_T}{B_T'} \right) \left[\left(\frac{V_0}{V} \right)^{B_T'} - 1 \right] \quad (1)$$

where B_T is the bulk modulus at zero pressure, and B_T' is the first derivative of B_T with pressure. The corresponding values for anthracene are $B_T = 7.484$ GPa and $B_T' = 7.345$.¹¹ Using eq 1, the experimentally applied pressure was related to the corresponding volume compression.

Using a standard definition for the mode Grüneisen parameter γ_i ,²⁶

$$\gamma_i = - \frac{d \ln (v_i)}{d \ln (V)} = - \frac{V (dv_i)}{v_i (dV)} \quad (2)$$

$$\frac{v_i(P)}{v_i(0)} = \left[\frac{V(0)}{V(P)} \right]^{\gamma_i} \quad (3)$$

where $v_i(P)$ is the vibrational frequency at an applied pressure

P , $V(P)$ is the volume of the bulk solid at pressure P , and γ_i is the Grüneisen parameter for vibrational mode i .

An accurate determination of mode Grüneisen parameters should be important for characterizing the mechanisms of shock-induced or solid-state detonation chemistry. A bulk, i.e., average, Grüneisen parameter can be used to model bulk thermodynamic changes associated with a shock, but such an analysis cannot describe nonequilibrium or mode-specific dynamics during the shock. Since chemical reactivity can depend exponentially on temperature, and the temperature of a shock wave can depend exponentially on the Grüneisen constant,^{27,28} mode specific chemical reactions are expected to be extremely sensitive to the mode Grüneisen parameters.

Pressure-induced Raman shifts of embedded microcrystals can also be used as a nanogauge for laser-induced shock wave studies.¹⁴ A summary of relevant shock wave basics and the use of anthracene as a nanogauge are discussed in detail in ref 14. For example, when an anthracene nanogauge is used with a PMMA polymer layer, the similar shock impedance (i.e., the acoustic velocity times the density²⁹) result in little reflection of the shock front at the interface.⁹

4. Results and Discussion

In the present study nitrogen was used as a hydrostatic pressure medium to alleviate problems associated with pressure-induced anthracene excimer defect emission. A previous Raman study of anthracene at high pressure reported that anthracene excimer defect emission dominated the Raman signal at pressures above 1.7 GPa.¹⁵ The use of nitrogen as a hydrostatic pressure-mediating fluid was found to eliminate defect emission over the 3.1 GPa pressure range of this study. Above 3.1 GPa, *photoinduced* fluorescent products or defects are observed which limit the pressure range of this study.

Raman spectra were taken at various pressures over the range 0–3.1 GPa. Typical spectra are shown in Figures 1 and 2. Figure 1 shows Raman spectra of anthracene in the frequency region 50–1100 cm⁻¹ at various pressures over the 0–3.1 GPa pressure range. Figure 2 shows Raman spectra of anthracene, in the frequency region 1100–1600 cm⁻¹, at various pressures over the 0–3.1 GPa pressure range. The pressure shifts of 15 Raman lines were analyzed over this pressure range. The six peaks below 200 cm⁻¹ at ambient pressure are external phonon modes, and the corresponding modes in perdeuterated anthracene have previously been studied up to a pressure of 0.8 GPa.⁸

4.1. Pressure-Induced Raman Shifts. A pressure-induced frequency increase was observed for all of the Raman modes studied. The pressure-induced shifts for the six phonon modes are plotted in Figure 3 and the corresponding shifts for the nine vibron modes are shown in Figure 4. The vibron modes in Figure 4 display a nearly linear shift with pressure, whereas the pressure-induced shift in the phonon frequencies shown in Figure 3 are nonlinear. The pressure-induced frequency shift results are summarized in Table 1. The vibrational modes listed in Table 1 are numbered and referenced by molecular symmetry;³⁰ however, the crystal symmetry splits these modes into a_g and b_g factor group components.

In all molecular materials the Raman frequency shifts and widths change with temperature and density. In a shock wave, the density can be converted to shock pressure⁶ when the Hugoniot is known. Although the specifics of density and temperature effects depend on details of the anharmonic intermolecular potential,⁷ which are difficult to calculate from first principles,⁸ empirical calibration of the high-pressure Raman spectrum⁹ enables the use of Raman spectroscopy to

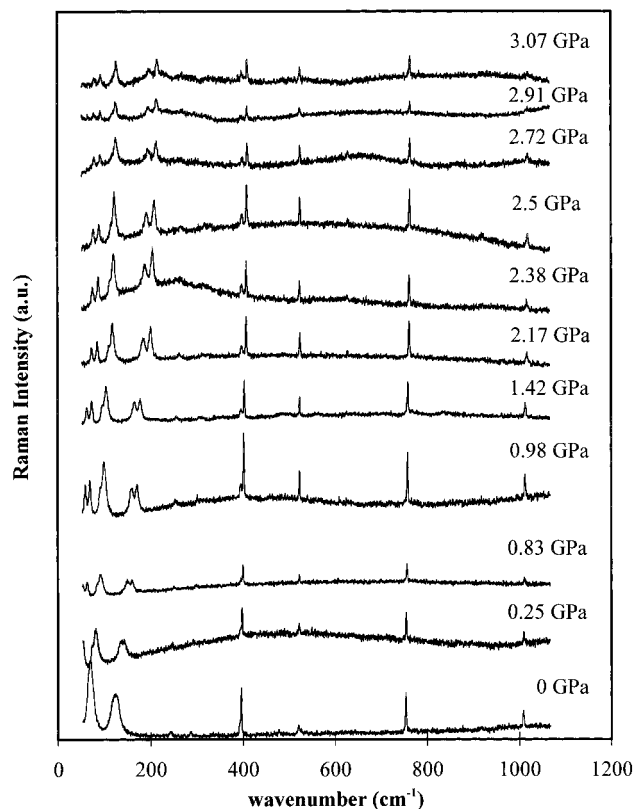


Figure 1. Raman spectra in the frequency range 50–1100 cm^{-1} at various pressures from 0 to 3.07 GPa.

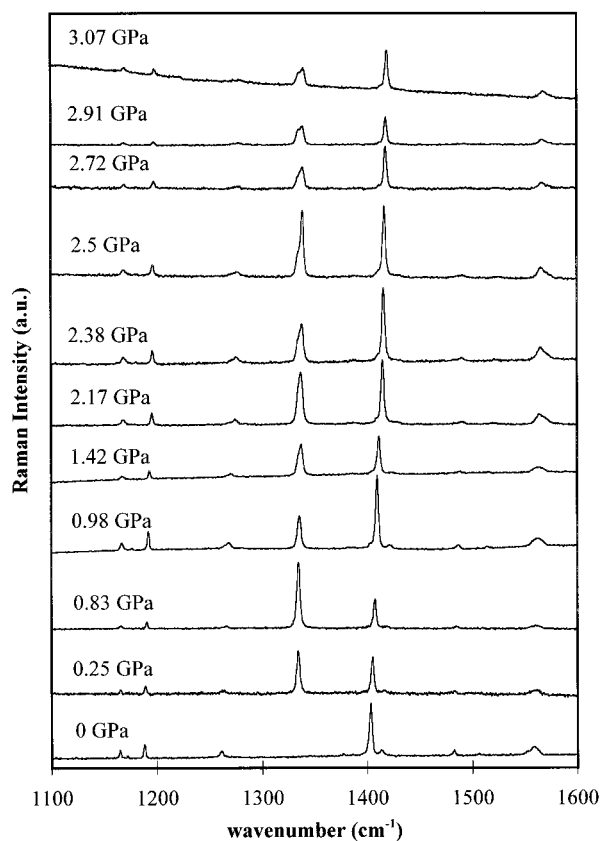


Figure 2. Raman spectra in the frequency range 1100–1600 cm^{-1} at various pressures from 0 to 3.07 GPa. The peaks near 1330 cm^{-1} are due to the diamond anvils of the high-pressure cell.

probe the temperature and pressure profile of materials and processes (e.g., laser-induced shock waves in molecular solids).⁹

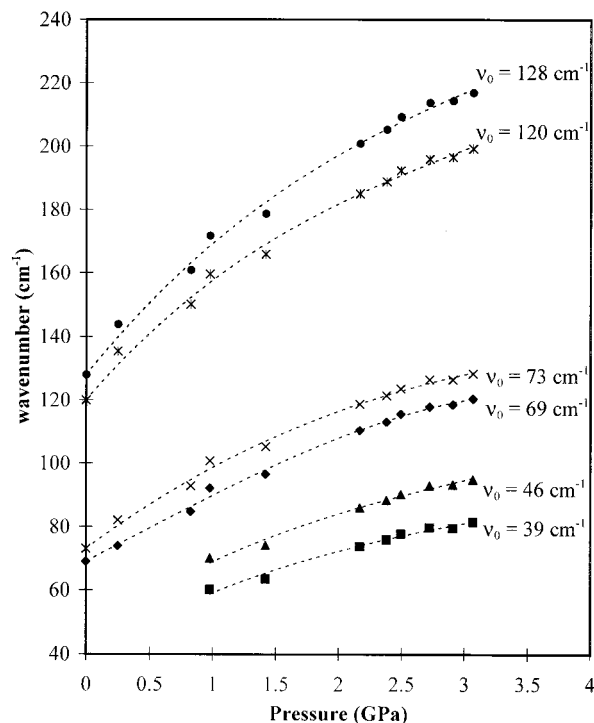


Figure 3. The pressure-induced Raman frequency shift of several of the phonons of crystalline anthracene.

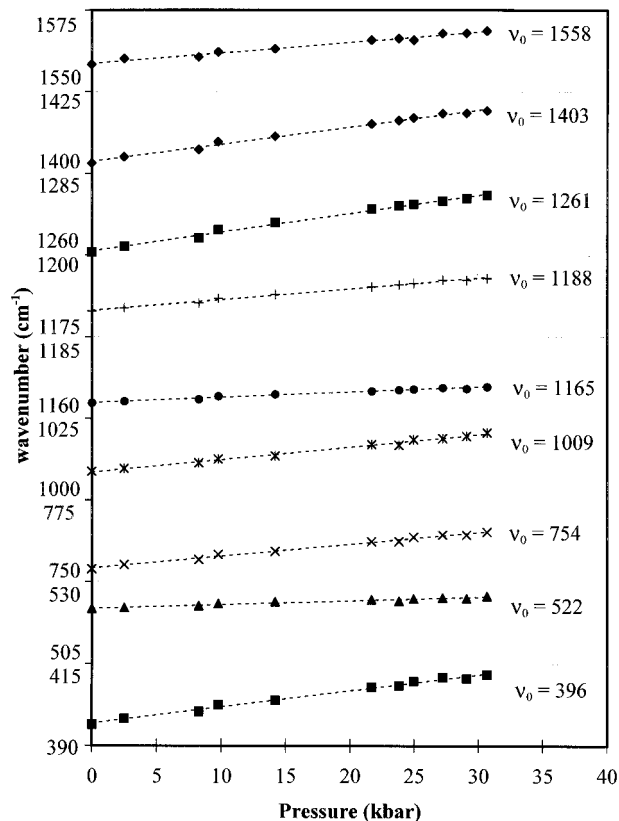


Figure 4. The pressure-induced Raman frequency shift of several of the vibrons of crystalline anthracene. The magnitude of the pressure-induced frequency shifts for the vibrons ranged from 1.5 to 5 cm^{-1} per GPa.

The present study calibrates 15 Raman transitions that can now be utilized for this purpose. The initial slopes of the pressure-induced frequency shifts for the different phonon modes were in the range 20–50 $\text{cm}^{-1}/\text{GPa}$ at ambient pressure, decreasing to 7–15 $\text{cm}^{-1}/\text{GPa}$ at 3.1 GPa, as shown in Figure 3. In contrast,

TABLE 1: Raman Shifts and Grüneisen Parameters

ν_0 (cm ⁻¹)	$\Delta\nu/\Delta P$ (cm ⁻¹ /GPa)	Grüneisen γ_i	mode assignment
39	<i>a</i>	4.01	a _g
46	<i>a</i>	4.00	b _g
69	<i>a</i>	2.96	b _g
73	<i>a</i>	3.06	a _g
120	<i>a</i>	2.78	a _g
128	<i>a</i>	2.87	b _g
396	5.0	0.186	12a _g
522	1.2	0.035	10b _{3g}
754	3.7	0.073	10a _g
1009	3.8	0.054	9a _g
1165	1.6	0.021	8a _g
1188	3.3	0.042	7b _{3g}
1261	5.7	0.068	7a _g
1403	5.2	0.057	6a _g
1558	3.2	0.031	4a _g

^a Non-linear pressure shifts are observed, as shown in Figure 3. The pressure-induced frequency shifts for the different phonon modes are in the range $\Delta\nu/\Delta P = 20$ to 50 cm⁻¹/GPa at ambient pressure, and decrease to $\Delta\nu/\Delta P = 7$ to 15 cm⁻¹/GPa at a pressure of 3.1 GPa.

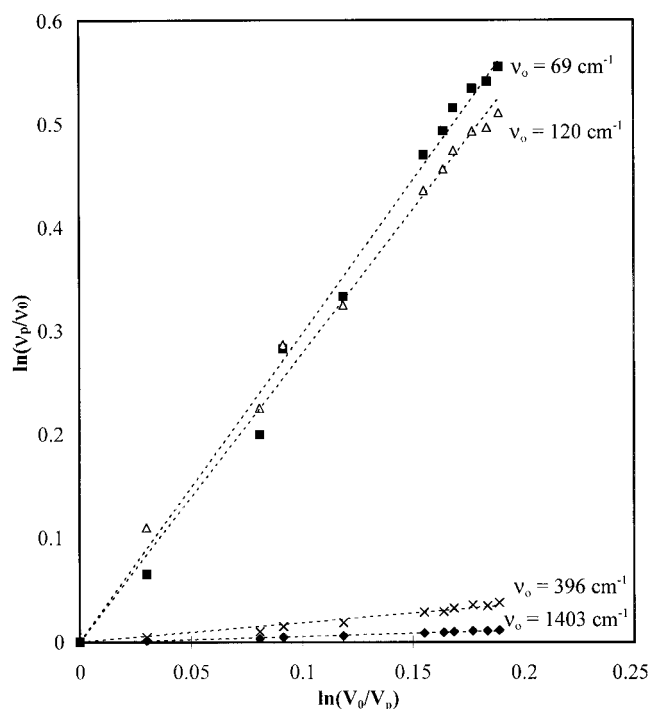


Figure 5. A log-log plot of the frequency ratio $\nu(P)/\nu(0)$ versus the volume ratio $V(0)/V(P)$ for representative Raman modes of anthracene. The slope of a linear fit to eq 1 yields the mode Grüneisen parameters, γ_i , listed in Table 1.

the intramolecular vibrons above 200 cm⁻¹ yielded fairly linear pressure shifts in the range 1.2 – 5.7 cm⁻¹/GPa, as shown in Figure 4. The 4-fold variation in the pressure shift values for the intramolecular modes can be important when considering vibrational shifts as a pressure gauge.⁹ Furthermore, some of the lower-frequency phonon modes near 130 cm⁻¹ (at ambient pressure) have Raman pressure shifts that, although nonlinear, can be nearly an order of magnitude greater than that of the 1403 cm⁻¹ vibron mode (ambient pressure) previously used for this purpose.⁹

4.2. Mode Grüneisen Parameters. The lattice compression given by eq 1 was used to generate the compression-induced shift data shown in Figure 5. The magnitude of mode Grüneisen constants indicate anharmonicity in the mode coordinate as well as differences between the local volume compression of the coordinate relative to the bulk volume compression.

TABLE 2: Changes in Raman Peak Widths at High Pressure

ν_0 (cm ⁻¹)	$\Delta\nu_{\text{FWHM}}(0\text{GPa})$ (cm ⁻¹)	$\Delta\nu_{\text{FWHM}}(3.1\text{GPa})$ (cm ⁻¹)
39		
46		
69		
73	12.7	7.7 ^a
120	16.3	13.8 ^a
128	16.2	10.2 ^a
396	2.0	3.3 ^b
522	7.6	5.4 ^a
754	2.5	3.4
1009	3.1	7.1 ^b
1165	2.0	4.0
1188	2.2	3.2
1261	3.9	11.3 ^b
1403	3.4	3.4
1558	9.2	8.2 ^a

^a Pressure-induced line narrowing. ^b Sudden increase in line width near 2.4 GPa. ^c The standard error in the $\Delta\nu_{\text{FWHM}}$ nonlinear least-squares fit parameter was 3%.

The compressibility of anthracene is well established¹¹ and is used to calculate the mode Grüneisen parameters, γ_i , for each vibration according to eq 3.^{26,31} If γ_i is nearly constant with volume,^{26,31} then a log-log plot of the relative frequency change versus the relative volume compression yields a linear fit with slope γ_i . Figure 5 shows representative plots of $\ln(\nu_P/\nu_0)$ versus $\ln(V_0/V_P)$ for two phonon modes and two vibron modes of anthracene along with linear least-squares fits to determine the mode Grüneisen parameters listed in Table 1. Since a purely harmonic mode would be volume independent (i.e. $\gamma = 0$), the magnitude of γ_i is a measure of the anharmonicity of the particular vibrational coordinate. The magnitudes of the γ_i values for the 15 Raman active modes summarized in Table 1 are typical of vibrations in molecular solids.

The relatively large γ values observed for intermolecular phonon modes are due to the relatively large compression of the vibrational coordinate, while the relatively small γ values observed for some intramolecular vibrons are due to the fact that compression occurs principally along intermolecular coordinates orthogonal to the vibron coordinate. Table 1 shows that there are some higher-frequency vibron coordinates with significant pressure-induced frequency shifts (e.g., ≥ 5 cm⁻¹/GPa for the 396, 1261, and 1403 cm⁻¹ modes). However, the proportional frequency shift for these higher-frequency modes is much less than for the intermolecular phonons, which gives rise to the vastly different mode Grüneisen values for the phonon ($\gamma_{\text{phonon}} \geq 2.8$) versus vibron ($\gamma_{\text{vibron}} \sim 0.1$) modes listed in Table 1.

4.3. Pressure-Dependent Raman Line Widths. The effect of pressure on the full width at half-maximum (FWHM) for some of the Raman peaks is shown in Figures 6 and 7 and the average change over the 0 to 3.1 GPa range is summarized in Table 2. In the absence of redundant samples at each pressure, the statistical noise in the Raman data yielded a standard error of 3% in the $\Delta\nu_{\text{FWHM}}$ nonlinear least-squares fit parameter. Although redundant spectra for different samples at the same pressure were not explicitly obtained, several different samples were studied utilizing nonmonotonic pressure changes, and no obvious hysteresis was observed. Simple trendlines have been drawn on Figures 6 and 7 as guides for the eye. For a few vibrons we observe that the FWHM of the peaks at 1261, 1009, and 396 cm⁻¹ broaden abruptly at a pressure near the proposed second-order phase transition pressure of 2.4 GPa, reported in a high-pressure IR study.¹⁶ In contrast to the IR study, we do

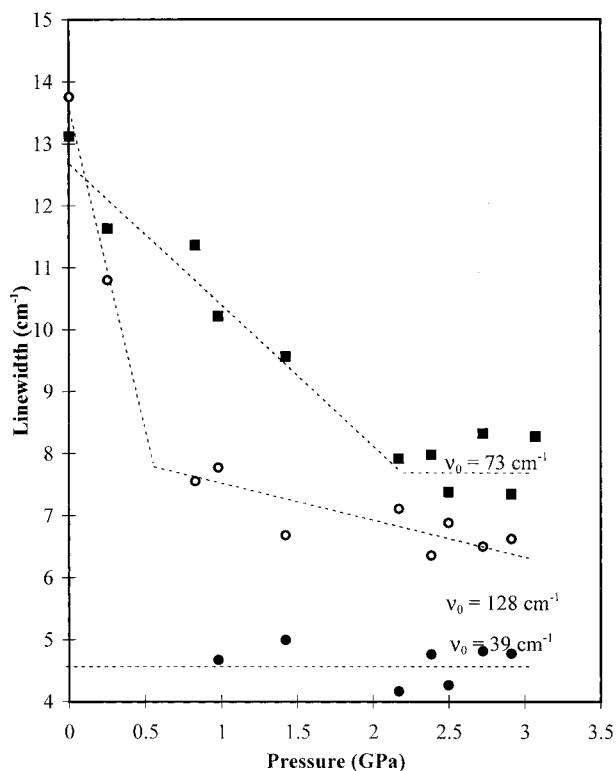


Figure 6. The pressure-induced change in Raman line widths (FWHM) for some of the phonons of crystalline anthracene. Raman lines with relatively large line widths at ambient pressure (i.e., 8–16 cm^{-1}) often showed pressure-induced line narrowing.

not observe any discontinuities in the Raman shifts as a function of pressure, only changes in the FWHM as discussed above.

We also observed pressure-induced line narrowing for several Raman phonon bands, especially those that are broadest at ambient pressure (e.g., 73 and 128 cm^{-1}), as illustrated in Figure 6. The pressure-induced line narrowing effect was also weakly observed for some vibron modes, as listed in Table 2.

The pressure-induced line narrowing illustrated in Figure 6 is comparable in magnitude to the line narrowing reported for the corresponding phonons of perdeuterated anthracene when the temperature was lowered from 300 to 200 K.⁸ The ratio $h\nu_{\text{phonon}}/kT$ can increase by a factor of 1.6 to 2 (depending on the phonon mode) by either a modest decrease in temperature (e.g., from 300 K down to 200 or 150 K) or by increasing the pressure over the 3.1 GPa range of this study. Thus, the pressure-induced line narrowing may reflect decreased homogeneous dephasing due to a decrease in phonon occupation numbers caused by the pressure-induced increase in phonon energies relative to kT . One cannot rule out the possibility that compression in a hydrostatic medium may also allow slight annealing of vibrational modes that were inhomogeneously broadened in the ambient pressure crystals.

Mode-specific inhomogeneous line width effects have also been documented in high-pressure vibronic relaxation studies of crystalline naphthalene.² Thus, it is possible that only a subset of the Raman active vibrons (e.g., those in Figure 7) would show inhomogeneous broadening induced by strain associated with the reported second-order polymorphic phase transition.¹⁶

5. Summary

The use of fluid nitrogen as a hydrostatic pressure medium alleviated the problem of pressure-induced defect fluorescence,¹⁵ enabling Raman spectra of crystalline anthracene to be obtained

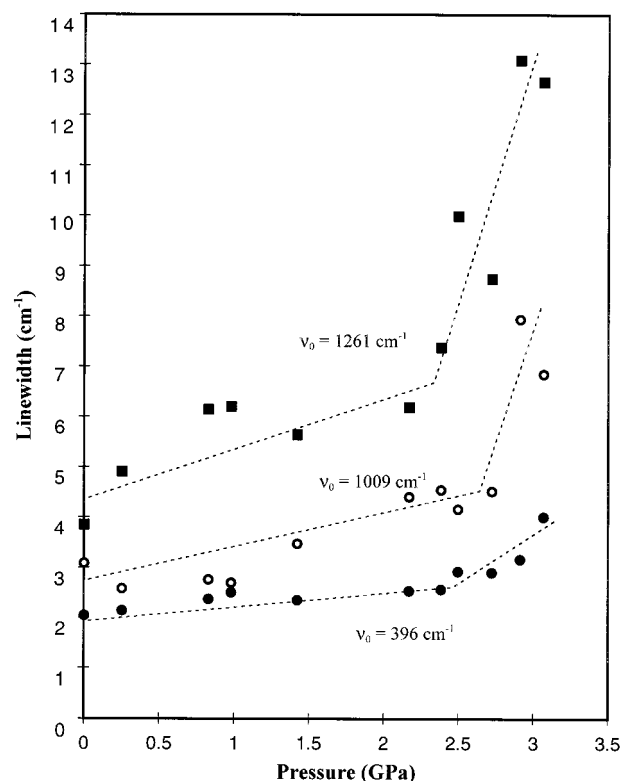


Figure 7. The pressure-induced change in Raman line widths for some vibrons of crystalline anthracene. The FWHM of the peaks at 1009 and 1262 cm^{-1} (and to a lesser extent 396 cm^{-1}) are observed to broaden abruptly at a pressures near 2.4 GPa, possibly due to a previously suggested second-order phase transition at this pressure.¹⁶

at pressures up to 3.1 GPa. The Raman spectrum is useful as a probe of chemical and physical changes in molecular solids, and the Raman spectrum of embedded anthracene microcrystals has been used as an empirical pressure and temperature gauge for molecular solids.⁹ Accurate pressure shift data was presented for six intermolecular phonon modes and nine intramolecular vibron modes of crystalline anthracene. The Raman modes with the greatest pressure shifts are of obvious value for use as a pressure gauge. An analysis of the Raman frequency shift relative to the volume compression of the anthracene lattice was also performed to determine mode Grüneisen parameters for 15 Raman modes. The resulting Grüneisen parameter values show a clear demarcation between the intramolecular phonon and the intermolecular vibron modes. Since chemical reactivity can depend exponentially on temperature, and the temperature of a shock wave can depend exponentially on the Grüneisen constant, chemical effects are expected to be extremely sensitive to the mode Grüneisen parameters.

Acknowledgment. We acknowledge the National Science Foundation (CHE-9714886) for financial support of this research.

References and Notes

- (1) Ferraro, J. R. *Vibrational Spectroscopy at High External Pressures*; Academic Press Inc.: New York, 1984, pp 2–3.
- (2) Crowell, R. A.; Chronister, E. L., *Chem. Phys. Lett.* **1992**, *195*, 602–607; Crowell, R. A.; Chronister, E. L. *J. Phys. Chem.* **1992**, *96*, 9660–9666.
- (3) Baer, B. J.; Chronister, E. L. *J. Phys. Chem.* **1995**, *99*, 7324–7329.
- (4) Lee, I.-Y. S.; Hare, D. E.; Hill, J. R.; Franken, J.; Suzuki, H.; Dlott, D. D.; Baer, B. J.; Chronister, E. L. In *Shock Compression of Condensed*

Matter; Schmidt, S. C. et al., Eds.; American Institute of Physics: New York, 1995; Vol 370, pp 905–908.

(5) D. Hare, E.; Dlott, D. D. In *Time-Resolved Vibrational Spectroscopy VII*; Woodruff, W., Ed.; Los Alamos Press: Los Alamos, 1995.

(6) Franken, J.; Hambir, S. A.; Hare, D. E.; Dlott, D. D. *Shock Waves* **1997**, *7*, 135.

(7) Califano, S.; Schettino, V.; Neto, N. *Lattice Dynamics of Molecular Crystals*; Springer-Verlag: Berlin, 1981.

(8) Häfner, W.; Kiefer, W. *J. Chem. Phys.* **1987**, *86*, 4582.

(9) Hambir, S.A.; Franken, J.; Hare, D. E.; Chronister, E. L.; Baer, B. J.; Dlott, D. D. *J. Appl. Phys.* **1997**, *81*, 2157.

(10) Kitaigorodsky, A. I. *Molecular Crystals and Molecules*; Academic: New York, 1973.

(11) Vaidya, S. N.; Kennedy, G. C. *J. Chem. Phys.* **1971**, *55*, 987.

(12) Warnes, R. H. *J. Chem. Phys.* **1970**, *53*, 1088.

(13) Schosser, C. L.; Dlott, D. D. *J. Chem. Phys.* **1984**, *80*, 1394.

(14) Dlott, D. D.; Hambir, S.; Franken, J. *J. Phys. Chem.* **1998**, *102*, 2121.

(15) Nicol, M.; Vernon, M.; Woo, J. T. *J. Chem. Phys.* **1975**, *63*, 1992.

(16) Adams, D. M.; Tan, T.-K. *J. Chem. Soc., Faraday Trans. 2* **1981**, *77*, 1711.

(17) Dows, D. A.; Hsu, L.; Mitra, S. S.; Brafman, O.; Hayek, M.; Daniels, W. B.; Crawford, R. K. *Chem. Phys. Lett.* **1973**, *22*, 595.

(18) Turrell, G. *Infrared and Raman Spectra of Crystals*; Academic: New York, 1972; p 38.

(19) Davydov, A. S. *Theory of Molecular Excitons*; Plenum: New York, 1971.

(20) Merrill, L.; Bassett, W. A. *Rev. Sci. Instrum.* **1974**, *45*, 290.

(21) Schiferl, D.; Cromer, D. T.; Mills, R. L. *High Temp. High Pressure Phys.* **1978**, *10*, 493.

(22) Piermarini, G. J.; Block, S.; Barnett, J. D.; Forman, R. A. *J. Appl. Phys.* **1975**, *46*, 2774.

(23) Barnett, J. D.; Block, S.; Piermarini, G. J. *Rev. Sci. Instrum.* **1973**, *44*, 1.

(24) Lowe, M.; Blumenroeder, S.; Kutt, P. H. *Comput. Phys. Commun.* **1988**, *50*, 367.

(25) Bevington, P. R. *Data Reduction and Error Analysis for the Physical Sciences*; McGraw-Hill: New York, 1969; p 159–162.

(26) Weinstein, B. A.; Zallen, R. In *Light Scattering in Solids IV*; Cardona, M., Güntherodt, G., Eds.; Springer-Verlag: Berlin, 1984; p 467.

(27) Tokmakoff, A.; Fayer, M. D.; Dlott, D. D. *J. Phys. Chem.* **1993**, *97*, 1901–1913.

(28) Nagayama, K. In *High-Pressure Science and Technology—1993*; Schmidt, S. C., Shaner, J. W., Samara, G. A., Ross, M., eds.; American Institute of Physics: New York, 1994; p 49.

(29) *LASL Shock Hugoniot Data*; Marsh, S. P., Ed.; University of California Press: Berkeley, CA, 1980.

(30) Jas, G.; Wan, C.; Kuczera, K.; Johnson, C. K. *J. Phys. Chem.* **1996**, *100*, 11857–11862; Zilberg, S.; Samuni, U.; Fraenkel, R.; Haas, Y. *Chem. Phys.* **1994**, *186*, 303–316.

(31) Born, M.; Huang, K. *Dynamical Theory of Crystal Lattices*; Oxford University Press: Oxford, 1954; pp 38–40.